An Experimental Study of Two-way Ranging Optimization in UWB-based Simultaneous Localization and Wall-Mapping Systems

Kai Li*, Wei Ni†, Bo Wei‡, and Mohsen Guizani§
*Real-Time and Embedded Computing Systems Research Centre (CISTER), Porto, Portugal.
Email: kai@isep.ipp.pt.
†Commonwealth Scientific and Industrial Research Organization (CSIRO), Sydney, Australia.
Email: wei.ni@data61.csiro.au.
‡Computer and Information Sciences, Northumbria University, UK.
Email: bo.wei@northumbria.ac.uk.
§Computer Science and Engineering Department, Qatar University, Doha, Qatar.
Email: mguizani@ieee.org.

2022 International Wireless Communications and Mobile Computing (IWCMC) | 978-1-6654-6749-0/22/$31.00 ©2022 IEEE | DOI: 10.1109/IWCMC55113.2022.9825332

***Abstract*—In this paper, we propose a new ultra-wideband (UWB)-based simultaneous localization and wall-mapping (SLAM) system, which adopts two-way ranging optimization on UWB anchor and tag nodes to track the target's real-time movement in an unknown area. The proposed UWB-based SLAM system captures time difference of arrival (TDoA) of the anchor nodes' signals over a line-of-sight propagation path and reflected paths. The real-time location of the UWB tag is estimated according to the real-time TDoA measurements. To minimize the estimation error resulting from background noise in the two-way ranging, a Least Squares Method is implemented to minimize the estimation error for the localization of a static target, while Kalman Filter is applied for the localization of a mobile target. An experimental testbed is built based on off-the-shelf UWB hardware. Experiments validate that a reflector, e.g., a wall, and the UWB tag can be located according to the two-way ranging measurement. The localization accuracy of the proposed SLAM system is also evaluated, where the difference between the estimated location and the ground truth trajectory is less than 1 meter.**

***Index Terms*—Ultra-wideband, Simultaneous localization and mapping, TDoA, Optimization, Experimental testbed**

I. Introduction

In recent years, precise indoor localization has been widely studied, which provides real-time tracking services in emergent scenarios, including military security, home surveillance, and medical supervision [1]. Thanks to small size, low cost, and high signal penetration, ultra-wideband (UWB) radio transceivers are used in wireless localization systems to track people or animal movements [2], [3]. In the UWB-based localization system, a UWB tag is attached to the tracking target, as shown in Fig. 1. A number of anchor nodes are deployed to cover an area of interest, such as walking paths in buildings or shops in shopping malls [4]. The anchor nodes are synchronized and continuously broadcast UWB signals. The UWB tag responds the captured UWB signal to the anchor node. Since the service area layout has considerable effects on signal reflection patterns and received signal strength of the UWB radio, localization accuracy of the UWB-based localization system greatly varies, which results in a unreliable localization service. Moreover, a priori knowledge of the floor plan and the radio pattern in the service area is often unknown. Hence, improving the localization accuracy of the UWB-based localization system in an unknown service area is not trivial.

In this paper, we propose a new UWB-based simultaneous localization and wall-mapping (SLAM) system to track the target's real-time movement in an unknown area. Specifically, two-way ranging is developed with the proposed UWB-based SLAM to capture the Time-Difference-of-Arrival (TDoA) of channel impulse response (CIR) signals [5], which are transmitted over a line-of-sight propagation path and reflected paths between the anchor nodes and the UWB tag. The real-time location of the UWB tag in the SLAM system is estimated according to the real-time TDoA measurements [6]. To minimize the estimation error resulting from background noise in the two-way ranging, a Least Squares Method [7] is implemented for the localization of a static target, while Kalman Filter [8] is applied for the localization of a mobile target.

Moreover, the proposed two-way ranging utilizes the TDoA of the UWB signal, as well as the localization of the UWB tag in the SLAM system, to determine boundaries of the service area, i.e., the location of walls in a room. Each anchor node is mapped to a virtual transmitter (VT) against the wall of the room. The distance between the VT and the UWB tag is regarded as the length of reflected path according to the wall. By calculating the TDoA of the VTs, the length of the wall can be estimated.

An experimental testbed is built based on off-the-shelf Decawave DWM1001 (a single UWB chip supported by the IEEE 802.15.4 standard) and a portable UWB kit, MDEK1001 [9]. Experiments are conducted in an anechoic

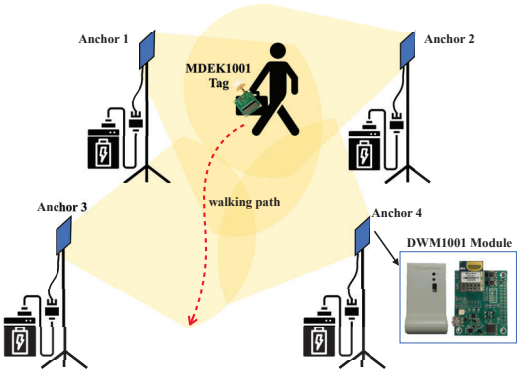

Fig. 1: In the UWB-based localization system, a UWB tag (e.g., MDEK1001) is attached to the tracking target, and a number of anchor nodes (e.g., DWM1001 made by Decawave) are deployed to cover an area of interest.

chamber at CSIRO, Australia, to measure the TDoA of the two-way ranging CIR values. The experiments validate that a signal reflector, e.g., the wall, can be detected according to the CIR measurement. In addition, the localization accuracy of the proposed SLAM system is evaluated, where the difference between the estimated location and the ground truth trajectory is less than 1 meter.

The rest of this paper is organized as follows. Section II presents the related work on wireless indoor localization. The system architecture and two-way ranging optimization in SLAM are illustrated in Section III. In Section IV, we implement the proposed SLAM system testbed with the two-way ranging optimization. Experiments are carried out to evaluate the localization performance. Finally, we conclude this work in Section V.

II. Related Work

In this section, we present the literature review on the existing indoor localization systems based on UWB, WiFi, camera, and motion sensors.

A UWB-based indoor localization system is developed in [10], where TDoA is applied with one way transmission ranging. Given unsynchronized anchors, the one-way transmission ranging is based on the timestamps collected at the anchors. The localization system implements a linear regression to predict next TDoA values of the packets transmitted by the tag. In [11], a leading-edge detection algorithm is studied for processing the UWB tag's requests in the localization system. A localization algorithm is developed to use two moving average windows to improve the accuracy detection of the UWB signals with low signal-to-noise ratios (SNRs) and non-line-of-sight (NLoS) conditions. A UWB-based indoor localization system is presented in [12], where the UWB tag can receive the responses from multiple anchors simultaneously. The tag calculates the TDoA value between the anchors and estimates the location of the tag itself, where the anchors are not required to be synchronized. Roetenberg *et al.* conduct a data fusion on the UWB and inertial measurements, which can track the human motions [13].

Although WiFi may not always achieve a satisfactory indoor localization performance, the SLAM systems combining motion sensors and WiFi can considerably improve the localization accuracy [14], [15]. One advantage of the WiFi-based localization solutions is the ubiquity of the WiFi devices in indoor environments. A WiFi protocol designing for the indoor localization, i.e., IEEE 802.11mc, has been released aiming for high-performance localization [16]. In [17] and [18], a lightweight people localization system is demonstrated, where a number of anchors are deployed to sniff probe requests periodically polled by targets' smartphones for WiFi connection. The target's presence is detected when the probe request of the smartphone is received by the anchor the target passes by. Therefore, the target's trajectory can be tracked by the probe requests on a series of anchors according to time. An indoor tracking system based on the probe requests broadcast by smartphones is developed in [19]. A probe request interval-based data collection scheme is presented, where the anchor extracts the source MAC address and timestamp from the probe request, and uploads the extracted data according to the probe request interval of the smartphone.

Camera- and laser-based methods [20], [21] can be used for the indoor localization thanks to the high-resolution measurements and high sampling rate. Due to the high energy consumption, powerful computing devices are usually required to process the image or video data for a high-quality localization. In [22], [23], radio signals are utilized for the device-free localization with the deployment of multiple access points. Moreover, the Localization systems based on magnetic induction devices along with motion sensors are tested to accelerate the system deployment process [24], [25]. The lighting change in the indoor environment or Bluetooth connections can also be explored for the SLAM system to improve the localization performance [26], [27].

III. The SLAM Localization System With Two-way Ranging

A. System architecture

Fig. 1 illustrates the proposed UWB-based SLAM system, where 4 Decawave DWM1001 anchor nodes are deployed and battery-powered MDEK1001 UWB tag is attached to the target. The anchors mounting at the same height communicate with the UWB tag in the same channel. Each anchor is connected to and powered by a laptop, where the two-way ranging optimization is conducted to compute the position of the tag. The anchor nodes periodically broadcast beacon messages for access request and information polling. The four anchor nodes initiate the two-way ranging with the UWB tag in time-division multiple access. The two-way ranging beacons contain the source and destination address, and a 16-bit checksum.

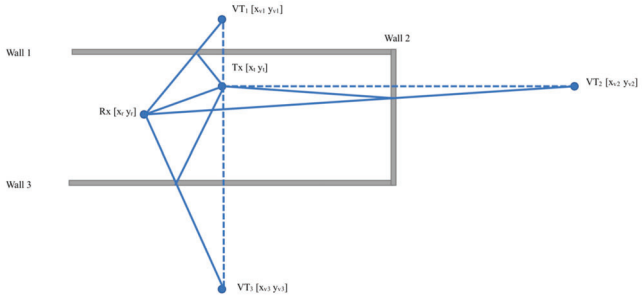

Fig. 2: Multipath reflection of the anchor node (the virtual transmitter) and the UWB tag.

To determine the boundary of the monitoring area, i.e., the walls, the proposed SLAM system investigates virtual transmitters (VT) that are geometrically symmetric to the tracked UWB tag corresponding to the wall. In particular, the distance between the UWB tag and a VT indicates the length of the reflected path, since the reflected path of the anchor node's signal can be regarded as a direct path between the VT and the tag. Fig. 2 studies an example for multipath reflection of the anchor node (the VT) and the UWB tag. Tx is the location of the anchor node and Rx is the location of the UWB tag. The VT's locations according to the three walls are denoted as VT_1, VT_2 and VT_3, respectively.

The coordinates of VT_1, VT_2 and VT_3 can be determined by

$$[x_v\ y_v] = [x_t\ y_t] - \frac{2\left([a\ b] \times \begin{bmatrix} x_t \\ y_t \end{bmatrix} + c\right)}{(a^2+b^2)} \times [a\ b] \quad (1)$$

where $[x_v\ y_v]$ is the location of the VT, and $[x_t\ y_t]$ is the location of the actual anchor node. a, b and c are the parameters of the straight-line equation of the wall, i.e., $ax + by + c = 0$.

The signal reflection is regarded as a line-of-sight (LoS) path and a reflected path. The LoS distance between the UWB tag and the anchor node can be obtained by

$$d_{TxRx} = \sqrt{(x_t - x_r)^2 + (y_t - y_r)^2} \quad (2)$$

The length of the reflected path is the distance between the locations of the actual anchor node and the VT. Given VT_1, VT_2, and VT_3, the length of the three reflected paths is

$$d_{RxVT_m} = \sqrt{(x_{vm} - x_r)^2 + (y_{vm} - y_r)^2}, \quad (3)$$

where m = 1, 2, or 3. Furthermore, the difference of the LoS and the reflected paths is

$$dT_m = \sqrt{(x_t - x_r)^2 + (y_t - y_r)^2} - \sqrt{(x_{vm} - x_r)^2 + (y_{vm} - y_r)^2} \quad (4)$$

where $m = 1, 2,$ or 3. Based on (4), the TDoA can be obtained by dT_m/c_l, where c_l is the speed of the light.

B. The SLAM system optimization

To minimize the estimation error of the walls' locations, we optimize the VT's position based on the Least Squares Method. With TDoA of the three reflection paths, we have

$$\min \sum_{i \in N, j \in M} \left(\Big\| \|VT_i - Rx_j\| - \|TX_v - Rx_j\| \Big\| - dT_m \right)^2 \quad (5)$$

where N and M are the numbers of anchor nodes and UWB tags, respectively. Based on the optimization in (5), the estimated distance between the anchor node and the wall is closest to the actual distance, which provides an accurate wall's location.

To track the UWB tag, the anchor node sends beacons to the tag every 0.3s, in other words, the location is sampled every 0.3s. The samples are taken as the input to a Kalman Filter. In particular, a location sample indicates the previous system state in the filter, which can be used to predict the current state. The following samples can be seen as observation values that correct the predicted current system state. The state of the UWB tag consists of its location and velocity, which can be represented as a matrix with two elements, $x_t = \begin{bmatrix} p_t \\ v_t \end{bmatrix}$, where p_t is the position of the tag and v_t is the velocity [28]. Hence, the previous state of x_t is given by

$$p_t = p_{t-1} + v_{t-1} \times \Delta t + u_t \times \frac{\Delta t^2}{2}, \quad (6)$$

$$v_t = v_{t-1} + u_t \times \Delta t, \quad (7)$$

where u_t is the velocity of the tag, and Δt is the time when the states are sampled. Furthermore, the system state can be given as a matrix:

$$\begin{bmatrix} p_t \\ v_t \end{bmatrix} = \begin{bmatrix} 1 & \Delta t \\ 0 & 1 \end{bmatrix} \begin{bmatrix} p_{t-1} \\ v_{t-1} \end{bmatrix} + \begin{bmatrix} \frac{\Delta t^2}{2} \\ \Delta t \end{bmatrix} u_t$$

We can observe the transformation matrix of Kalman Filter, which gives $F_t = \begin{bmatrix} 1 & \Delta t \\ 0 & 1 \end{bmatrix}$. The control matrix that illustrates how the controlled variable u_t acts on the current state is $B_t = \begin{bmatrix} \frac{\Delta t^2}{2} \\ \Delta t \end{bmatrix}$.

Let "$\hat{}$" denote the estimated value, and " $^-$ " denote the value that is predicted optimally in accordance with the previous state. Predicting the current state in Kalman Filter can be formulated as

$$\widehat{x_t}^- = F_t \widehat{x}_{t-1} + B_t u_t. \quad (8)$$

Moreover, sampling noise results in uncertainties on the state's prediction. A covariance matrix that calculates the correlation between the states can quantify the uncertainty of the prediction. The covariance matrix comes from the process noise and propagation of the uncertain predicted state. Based on the property of the covariance matrix, i.e.,

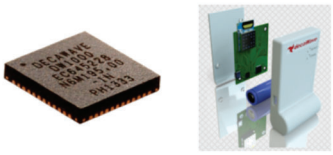

(a) Hardware of the off-the-shelf Decawave DW1000 chip.

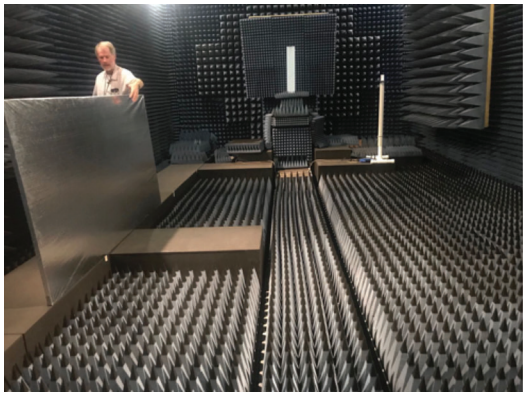

(b) CIR measurements in the indoor anechoic chamber.

Fig. 3: Experiments based on our SLAM testbed are conducted to characterize the CIR measurements in an anechoic chamber at CSIRO, Australia.

$cov\left(Ax, By\right) = A cov\left(x, x\right) B^T$, the covariance matrix prediction is formulated as

$$P_t^- = F P_{t-1} F^T + Q, \tag{9}$$

where Q is the covariance matrix of the sampling noise.

The signal measurements are the observations z_t, which yields

$$z_t = H x_t + v, \tag{10}$$

where H is the observation model matrix, and v is the measurement noise of the observation. Let K_t denote the Kalman filter, which is

$$K_t = P_t^- H^T \left(H P_t^- H^T + R\right)^{-1} \tag{11}$$

where R is the noise.

We define a measurement residual as the difference of the observation and the estimated value, namely, $z_t - H\widehat{x_t}^-$. With the obtained prediction state $\widehat{x_t}^-$, the measurement residual and Kalman factor can be used to correct the prediction state, which gives

$$\widehat{x_t} = \widehat{x_t}^- + K_t \left(z_t - H\widehat{x_t}^-\right). \tag{12}$$

The noise distribution of the optimal estimation is updated for next iteration by using

$$P_t = \left(I - K_t H\right) P_t^-. \tag{13}$$

IV. The SLAM Testbed and Experiments

In this section, we first demonstrate the experimental testbed which is built based on the off-the-shelf Decawave DWM1001 UWB kit. Next, experiments are carried out to measure CIR values in the indoor anechoic chamber, and track the UWB tag's movement.

A. UWB measurements in the indoor anechoic chamber

In our SLAM testbed, a number of anchor nodes are deployed to cover an indoor area. The anchor nodes are synchronized and continuously broadcast UWB signals. The UWB tag that is attached to a person responds the anchor nodes. The anchor nodes and the tag are developed with the off-the-shelf Decawave DW1000 chip and MDEK1001 kit, as shown in Fig. 3(a).

Based on the SLAM testbed, we carry out experiments to characterize the CIR measurement in an anechoic chamber at CSIRO, Australia, which is shown in Fig. 3(b). The experiments aim to capture features of the CIR strength variation according to the location of the obstacle. The localization with the Least Squares Method and Kalman Filter is implemented in Python, which carries out the two-way ranging to determine the UWB tag's location. A metal panel is placed as the signal reflector in the field, which leads to a multi-path signal reflection on the transmitted UWB signal of the anchor node. Moreover, Fig. 4 demonstrates the setup of the anchor node, UWB tag and the reflector in the chamber. Specifically, the distance between the anchor node and the tag is about 7.010 meters. The distances from the metal panel to the anchor and the tag are about 4.699 and 4.547 meters, respectively. Thanks to the signal absorption, the CIR in the chamber can experience two paths, one is the LoS link between the anchor and the tag, and the other is the reflected signal by the panel.

Fig. 5 presents the collected data samples regarding the CIR strength value in the chamber. Due to the LoS signal and the reflected one from the metal panel, we can observe the two highest peaks of the CIR measurement. The Time-of-Arrival (ToA) of the LoS signal is 747ns and that of the reflected one is 754ns. Hence, the experimental TDoA between the LoS signal and the reflected one is about 7ns. Given the speed of signal transmission about 2.99×10^8m/s, the distance difference between the anchor and the tag, and the anchor and the metal panel can be estimated

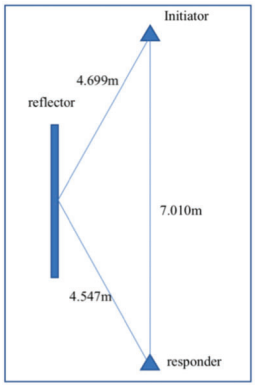

Fig. 4: The setup of the anchor node, UWB tag and the reflector.

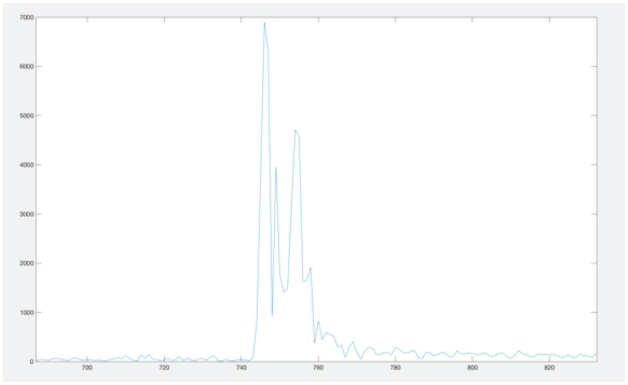

Fig. 5: CIR measurements based on the SLAM testbed.

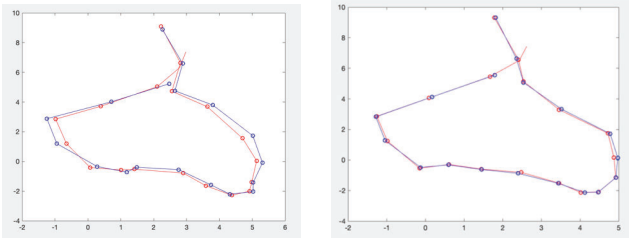

(a) (b)

Fig. 6: Performance comparison, where the ground truth trajectory is marked red line. The blue line in (a) stands for the localization based on the CIR measurement without the Least Squares Method and Kalman Filter, and the one in (b) is the proposed localization optimization.

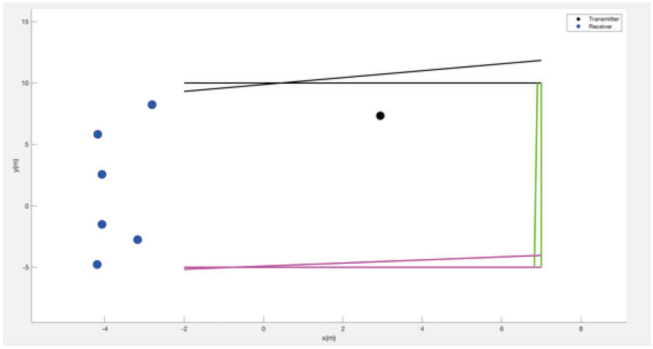

Fig. 7: The two-way ranging CIR measurement for the walls' localization, where 6 anchor nodes are placed in the field.

by 2.99 $\times$ 10^8m/s $\times$ 7ns = 2.09m. Given the measured distances 4.699m and 4.547m, the distance between the anchor node and the tag can be estimated as (4.699m + 4.547m) - 2.09m = 7.156m. Compared to the measured distance 7.010m, the estimation error is only 14.6cm, which validates the reliability of the proposed localization optimization.

B. Localization performance

Fig. 6 compares the localization performance of the proposed optimization with the Least Squares Method and Kalman Filter and the one without the Kalman Filter. In particular, Fig. 6(a) shows that the localization without the Kalman Filter is at most 50cm away from the ground truth which is marked red. Given a total of 19 waypoints, only 4 of them are tracked. Fig. 6(b) shows that Kalman Filter highly reduces the localization error below 15cm, while 14 of the 19 waypoints are successfully tracked.

As shown in Fig. 7, the proposed SLAM system estimates the location of the three walls based on the two-way ranging CIR measurement. The three walls are in a rectangle shape, where 6 anchor nodes are placed in the filed. Thanks to the Least Squares Method, our SLAM system achieves the localization error below 2 meters on the wall detection.

In Fig. 8, the proposed SLAM system adapts the Least Squares Method and Kalman Filter to estimate the location of the three walls (marked by a red dash line) while tracking the trajectory of the UWB tag (which is the green line). Since the location is sampled every 0.3s, we also plot several sample values which are the blue dots in the figure. Based on the samples, the proposed localization estimates the trajectory of the UWB tag. As observed, the trajectory is effectively tracked along the ground truth (i.e., the pink line).

V. Conclusion

In this paper, we demonstrated a new UWB-based SLAM system to track the target's real-time movement in an unknown area. The proposed UWB-based SLAM system captures the TDoA of the anchor nodes' signals over an LoS propagation path and reflected paths. The real-time location of the UWB tag is estimated according to the real-time TDoA measurements. The Least Squares Method and Kalman Filter are developed in the proposed SLAM system to minimize the estimation error resulting from the background noise in the two-way ranging. An experimental testbed is built based on off-the-shelf UWB hardware. Experiments validate that the wall and the UWB tag can

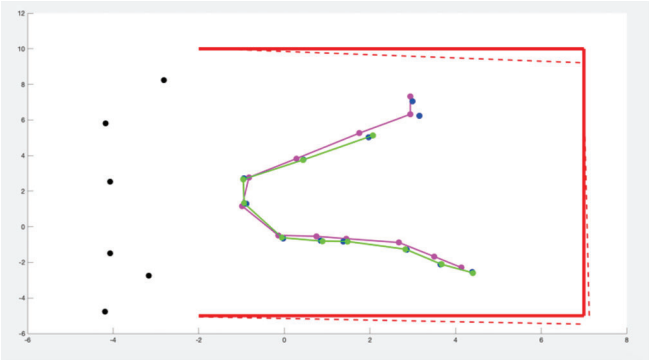

Fig. 8: The proposed SLAM system achieve the localization of the walls and the UWB tag.

be located according to the two-way ranging CIR measurement. The localization accuracy of the SLAM system is evaluated, where the difference between the estimated location and the ground truth trajectory is less than 15cm.

REFERENCES

[1] F. Gu, X. Hu, M. Ramezani, D. Acharya, K. Khoshelham, S. Valaee, and J. Shang, "Indoor localization improved by spatial context—a survey," *ACM Computing Surveys (CSUR)*, vol. 52, no. 3, pp. 1–35, 2019.

[2] M. Ridolfi, A. Kaya, R. Berkvens, M. Weyn, W. Joseph, and E. D. Poorter, "Self-calibration and collaborative localization for UWB positioning systems: A survey and future research directions," *ACM Computing Surveys (CSUR)*, vol. 54, no. 4, pp. 1–27, 2021.

[3] F. Zafari, A. Gkelias, and K. K. Leung, "A survey of indoor localization systems and technologies," *IEEE Communications Surveys & Tutorials*, vol. 21, no. 3, pp. 2568–2599, 2019.

[4] T. Kagawa, H.-B. Li, and R. Miura, "A uwb navigation system aided by sensor-based autonomous algorithm-deployment and experiment in shopping mall," in *2014 International Symposium on Wireless Personal Multimedia Communications (WPMC)*. IEEE, 2014, pp. 613–617.

[5] C. Jiang, S. Chen, Y. Chen, D. Liu, and Y. Bo, "An UWB channel impulse response de-noising method for NLOS/LOS classification boosting," *IEEE Communications Letters*, vol. 24, no. 11, pp. 2513–2517, 2020.

[6] J. Xu, M. Ma, and C. Law, "Performance of time-difference-of-arrival ultra wideband indoor localisation," *IET science, measurement & technology*, vol. 5, no. 2, pp. 46–53, 2011.

[7] S. Bolognani, S. Del Favero, L. Schenato, and D. Varagnolo, "Consensus-based distributed sensor calibration and least-square parameter identification in WSNs," *International Journal of Robust and Nonlinear Control: IFAC-Affiliated Journal*, vol. 20, no. 2, pp. 176–193, 2010.

[8] G. F. Welch, "Kalman filter," *Computer Vision: A Reference Guide*, pp. 1–3, 2020.

[9] R. Simedroni, E. Puschita, T. Palade, P. Dolea, C. Codau, R. Buta, and A. Pastrav, "Indoor positioning using decawave MDEK1001," in *International Workshop on Antenna Technology (iWAT)*. IEEE, 2020, pp. 1–4.

[10] J. J. Pérez-Solano, S. Ezpeleta, and J. M. Claver, "Indoor localization using time difference of arrival with uwb signals and unsynchronized devices," *Ad Hoc Networks*, vol. 99, p. 102067, 2020.

[11] M. J. Kuhn, J. Turnmire, M. R. Mahfouz, and A. E. Fathy, "Adaptive leading-edge detection in uwb indoor localization," in *2010 IEEE Radio and Wireless Symposium (RWS)*. IEEE, 2010, pp. 268–271.

[12] B. Großwindhager, M. Stocker, M. Rath, C. A. Boano, and K. Römer, "Snaploc: An ultra-fast uwb-based indoor localization system for an unlimited number of tags," in *Proceedings of the 18th International Conference on Information Processing in Sensor Networks*, 2019, pp. 61–72.

[13] D. Roetenberg, H. Luinge, and P. Slycke, "Xsens MVN: Full 6DOF human motion tracking using miniature inertial sensors," *Xsens Motion Technologies BV, Tech. Rep*, vol. 1, pp. 1–7, 2009.

[14] B. Ferris, D. Fox, and N. D. Lawrence, "Wifi-slam using gaussian process latent variable models." in *IJCAI*, vol. 7, no. 1, 2007, pp. 2480–2485.

[15] J. Huang, D. Millman, M. Quigley, D. Stavens, S. Thrun, and A. Aggarwal, "Efficient, generalized indoor wifi graphslam," in *IEEE international conference on robotics and automation*. IEEE, 2011, pp. 1038–1043.

[16] B. P. Crow, I. Widjaja, J. G. Kim, and P. T. Sakai, "IEEE 802.11 wireless local area networks," *IEEE Communications magazine*, vol. 35, no. 9, pp. 116–126, 1997.

[17] K. Li, C. Yuen, S. S. Kanhere, K. Hu, W. Zhang, F. Jiang, and X. Liu, "An experimental study for tracking crowd in smart cities," *IEEE Systems Journal*, vol. 13, no. 3, pp. 2966–2977, 2018.

[18] K. Li, C. Yuen, and S. Kanhere, "Senseflow: An experimental study of people tracking," in *Proceedings of the 6th ACM Workshop on Real World Wireless Sensor Networks*, 2015, pp. 31–34.

[19] K. Li, C. Yuen, S. S. Kanhere, K. Hu, W. Zhang, F. Jiang, and X. Liu, "Understanding crowd density with a smartphone sensing system," in *2018 IEEE 4th World Forum on Internet of Things (WF-IoT)*. IEEE, 2018, pp. 517–522.

[20] E. S. Jones and S. Soatto, "Visual-inertial navigation, mapping and localization: A scalable real-time causal approach," *The International Journal of Robotics Research*, vol. 30, no. 4, pp. 407–430, 2011.

[21] J. A. Hesch, F. M. Mirzaei, G. L. Mariottini, and S. I. Roumeliotis, "A laser-aided inertial navigation system (l-ins) for human localization in unknown indoor environments," in *2010 IEEE International Conference on Robotics and Automation*. IEEE, 2010, pp. 5376–5382.

[22] B. Wei, A. Varshney, N. Patwari, W. Hu, T. Voigt, and C. T. Chou, "drti: Directional radio tomographic imaging," in *Proceedings of the 14th International Conference on Information Processing in Sensor Networks*, 2015, pp. 166–177.

[23] J. Wilson and N. Patwari, "Radio tomographic imaging with wireless networks," *IEEE Transactions on Mobile Computing*, vol. 9, no. 5, pp. 621–632, 2010.

[24] B. Wei, N. Trigoni, and A. Markham, "iMag: Accurate and rapidly deployable inertial magneto-inductive localisation," in *IEEE International Conference on Robotics and Automation (ICRA)*. IEEE, 2018, pp. 99–106.

[25] B. Wei, N. Trigoni, and A. Markham, "iMag+: An accurate and rapidly deployable inertial magneto-inductive SLAM system," *IEEE Transactions on Mobile Computing*, 2021.

[26] B. Wei, W. Xu, C. Luo, G. Zoppi, D. Ma, and S. Wang, "SolarSLAM: Battery-free loop closure for indoor localisation," in *IEEE/RSJ International Conference on Intelligent Robots and Systems (IROS)*. IEEE, 2020, pp. 4485–4490.

[27] G. Ionescu, C. M. de la Osa, and M. Deriaz, "Improving distance estimation in object localisation with bluetooth low energy," *SENSORCOMM*, vol. 2014, pp. 45–50, 2014.

[28] Y. Zou and H. Liu, "TDOA localization with unknown signal propagation speed and sensor position errors," *IEEE Communications Letters*, vol. 24, no. 5, pp. 1024–1027, 2020.